Experimental Animals
Exp. Anim. 70(3), 344–354, 2021

Original

Repair of brain damage size and recovery of neurological dysfunction after ischemic stroke are different between strains in mice: evaluation using a novel ischemic stroke model

Yasuki MATANO[1)], Yuuto NOJIRI[1)], Mizuki NOMURA[1)], Akira MASUDA[1)], Yuuki MORIIKE[1)], Yasuhiro SUZUKI[2)], Kazuo UMEMURA[3)] and Nobuo NAGAI[1)]

[1)]*Laboratory of Animal Physiology, Division of Bioscience, Nagahama Institute of Bio-Science and Technology, 1266 Tamura, Nagahama, Shiga 526-0829, Japan*
[2)]*School of Pharmaceutical Sciences, Faculty of Pharmacy, Ohu University, 31-1 Sankaku-do, Tomita-cho, Kohriyama, Fukushima 963-8611, Japan*
[3)]*Department of Pharmacology, Hamamatsu University School of Medicine, 1-20-1 Handa-yama, Higashi-ku, Hamamatsu, Shizuoka 431-3125, Japan*

Abstract: In the current study, we established a novel murine ischemic brain damage model using a photochemical reaction to evaluate the recovery of neurological dysfunction and brain repair reactions. In this model, reproducible damage was induced in the frontal lobe of the cortex, which was accompanied by neurological dysfunction. Sequential changes in damage size, microglial accumulation, astrocyte activation, and neurological dysfunction were studied in C57BL/6J and BALB/c mouse strains. Although the initial size of damage was comparable in both strains, the extent of damage was later reduced to a greater extent in C57BL/6J mice than that in BALB/c mice. In addition, C57BL/6J mice showed later edema clearance until day 7, less microglial accumulation, and relatively more astrocyte activation on day 7. Neurologic dysfunction was evaluated by three behavioral tests: the von Frey test, the balance beam test, and the tail suspension test. The behavioral abnormalities evaluated by these tests were remarkable following the induction of damage and recovered by day 21 in both strains. However, the abnormalities were more prominent and the recovery was later in C57BL/6J mice. These findings demonstrate that our novel ischemic stroke model is useful for evaluating brain repair reactions and the recovery of neurological dysfunction in mice with different genetic backgrounds. In addition, we found that both the brain repair reactions and the recovery of neurological dysfunction after comparable ischemic brain damage varied between strains; in that, they both occurred later in C57BL/6J mice.
Key words: edema, ischemic stroke, microglia, neurological dysfunction, strains

Introduction

Although various animal models of ischemic brain damage have been established [1–3] the size and region of induced damage vary considerably among individual animals, strains (including C57BL/6J and BALB/c) [4–6], and transgenic/knockout animals with different genetic backgrounds [7, 8]. Here we established an ischemic brain damage model in which the damage was induced by photochemically-induced thrombosis (PIT) in the parietal lobe of the cortex (PIT-P model). This model demonstrates high reproducibility in terms of both the area and region of damage; that is, the difference between individual animals and different strains was low [5]. In addition, we showed that the difference in the initial amount of damage affected the intensity of sub-

(Received 30 November 2020 / Accepted 2 March 2021 / Published online in J-STAGE 16 March 2021)
Corresponding author: N. Nagai. e-mail: n_nagai@nagahama-i-bio.ac.jp

sequent repair responses; that is, a larger size of damage elicited stronger repair responses [5]. These results suggest that repair responses should be compared between animals with comparable amounts of brain damage in stroke. Thus, the existing models, in which the size and region of damage show relatively large variation, are unsuitable for studying repair responses.

Given that the damage induced in the PIT-P model is not accompanied by behavioral abnormalities, it is unsuitable for assessing the recovery of neurological dysfunction. Therefore, we attempted to establish a new stroke model in which reproducible damage is induced in the motor and sensory areas in the frontal lobe of the cortex using PIT method (PIT-F model). Furthermore, we also compared the changes in damage size and pathophysiological responses, including microglial accumulation and glial scar formation, under histological observation at low magnification. Finally, we used three behavioral tests to examine any differences in neurological dysfunction between C57BL/6J and BALB/c mice after brain damage using the PIT-F model.

Materials and Methods

All animal experimental procedures were approved by the Committee on Animal Care and Use of the Nagahama Institute of Bio-Science and Technology (Permit Number: 017). Animal studies were performed in accordance with institutional and national guidelines and regulations and the ARRIVE (Animal Research: Reporting of *In Vivo* Experiments) guidelines (https://www.nc3rs.org.uk/arrive-guidelines).

In all experiments, 37 male C57BL/6J mice (CLEA Japan, Tokyo, Japan) and 34 male BALB/c mice (CLEA Japan), 12–16 weeks old and weighing 25–34 g, were used. The number of animals used in each experiment is described in the figure legends.

Ischemic brain injury was induced using the PIT method [5, 9] with some modifications. Briefly, under isoflurane anesthesia, mice were placed on a heated pad maintained at 37°C, and a cannula was inserted into the left jugular vein. The skin on the top of the head was incised, and an optic fiber (1.0-mm diameter) was placed directly on the surface of the skull at the frontal lobe (bregma–lambda=0.0 mm, lateral=3.0 mm to the left). Immediately after infusion of 20 mg/kg Rose Bengal (Wako Pure Chemicals, Osaka, Japan), the areas were illuminated with a green light (wavelength, 540 nm; illumination intensity, 4.7×10^{-4} W/cm^2) through the optic fiber for 10 min using a light source (model L5178; Hamamatsu Photonics, Hamamatsu, Japan). After illumination, the cannula was withdrawn, and the skin was sutured.

To analyze the initial area of damage, the mice were deeply anesthetized with 200 mg/kg of secobarbital sodium solution (Nichi-Iko Pharmaceutical Co., Toyama, Japan), and the brains were removed after 24 h (day 1). The brains were then stained with 2,3,5-triphenyltetrazolium chloride (TTC), either directly or after being divided into 6 slices each at 1-mm thickness (Fig. 1) [8].

Histological analysis was performed as described elsewhere, with some modifications [5, 9]. Briefly, mice were perfused with saline and fixed with 4% paraformaldehyde under the euthanasia procedure using deep anesthetization with secobarbital sodium. The brains of the mice were removed 1, 4, 7, 14, and 21 days after stroke. The size of the damaged area was measured on the photograph of the brain surface, taken at a 45° angle (Fig. 2D). Then, the brains were sectioned into six 1 thick slices. Each slice was embedded in OCT compound

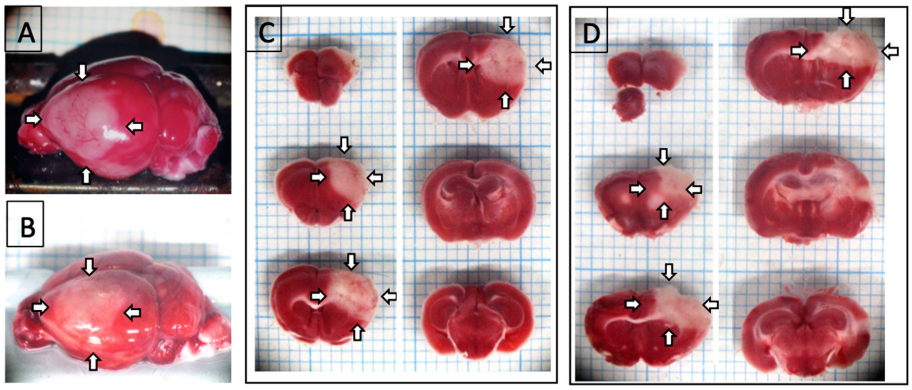

Fig. 1. Region of brain damage in the PIT-F model. A and B: Photographs of the TTC-stained brain surface of C57BL/6J mice (A) and BALB/c mice (B) on day 1. C and D: Specimen photomicrographs of TTC-stained 1-mm thick brain slices of C57BL/6J mice (C) and BALB/c mice (D). White regions indicated by arrows are damaged regions. Comparable results were obtained in 6 C57BL/6J mice and 4 BALB/c mice. The width of the grid behind the brain and sections was 1 mm.

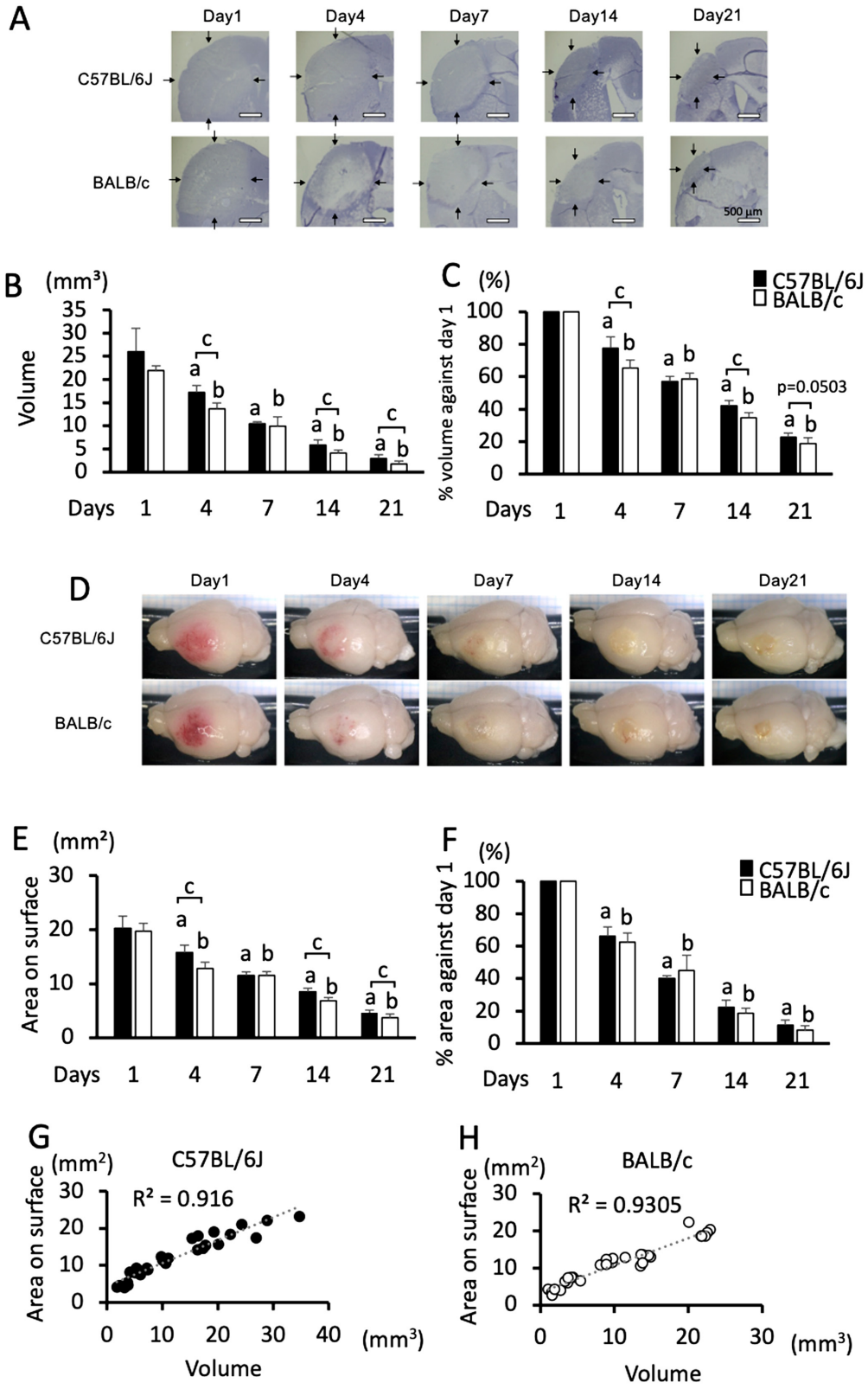

Fig. 2. Sequential changes in the size of damage in C57BL/6J and BALB/c mice in the PIT-F model. A: Specimen photomicrographs of the center of damage in the sections of C57BL/6J and BALB/c mice on days 1, 4, 7, 14, and 21. Arrows indicate areas of damage; bars indicate 500 μm. B and C: Sequential changes in the area of damage in terms of volume (B) and percentage of volume against day 1 (C). D: Specimen photomicrographs of damage on the surface of C57BL/6J and BALB/c mice on days 1, 4, 7, 14, and 21. Sequential changes of damage size measured on the area of the brain surface (E) and percentage of the area against day 1 (F). Data represent the mean and SD. a: $P<0.05$ vs. day 1 in C57BL/6J mice, b: $P<0.05$ vs. day 1 in BALB/c mice, c: $P<0.05$ comparison between C57BL/6J and BALB/c mice. G and H: Correlations between damage volume and damage size on the brain surface in C57BL/6J mice (G) and BALB/c mice (H). The correlation coefficient (R^2) is shown in each graph. n=6, 7, 5, 7, and 6 C57BL/6J mice, and n=6, 6, 6, 7, and 5 BALB/c mice were used on days 1, 4, 7, 14, and 21, respectively.

 doi: 10.1538/expanim.20-0182

(Sakura Finetek Japan, Tokyo, Japan), and 5-μm thick sections were cut from the rostral edge in frozen conditions prior to staining with hematoxylin (Fig. 2C). The volume of brain damage was calculated by multiplying the sum of the damage area in each section obtained from six brain slices by the thickness of slices (1 mm). In addition, the ratio of the size of damage in terms of volume and area on the surface against day 1 was also calculated.

The net damage volume and edema volume were measured in hematoxylin & eosin-stained sections. The brain damage volume is defined as the net brain damage volume indicating the volume of damage of the brain parenchyma and the edema volume, which is swelling of damaged tissue. After taking photographs, the areas of damage (Fig. 3C, Area-X), the ipsilateral alive area (Fig 3C, Area-Y), and the contralateral area (Fig. 3C, Area-Z) were measured. The net damage volume was calculated by multiplying the sum of the net damage area, which was calculated by subtracting the contralateral area from the ipsilateral alive area (Z − Y) in each section obtained from the six brain slices by the slice thickness (1 mm). The volume of edema was calculated by multiplying the sum of the enlargement of the ipsilateral area against the contralateral area calculated by X + Y − Z in each section obtained from six brain slices in a 1 mm^2 thickness by their thickness (1 mm) [10]. Both the ratio of the volume of edema against the volume of day 1 and the edema volume indicated as the ratio against the ipsilateral hemisphere area calculated by (X + Y − Z) / Z in percentage were also measured. The sequential change in the amount of striatum damage was also evaluated in terms of volume and percentage of the whole striatum area.

For immunohistochemistry, sections obtained from the center of damage were incubated with anti-F4/80 antibody (Abcam, Tokyo, Japan) or anti-GFAP antibody (Diagnostic Biosystems, Pleasanton, CA, USA). After treatment with an appropriate secondary antibody conjugated with Cy3 or fluorescein, the damaged area on the sections (Fig. 4A) was imaged by fluorescence microscopy (BX53; Olympus, Tokyo, Japan). Then, the thickness of the F4/80- or GFAP-positive layer was measured. The thickness of the F4/80-positive layer was measured by the average of three individual points surrounding the damage. The thickness of the GFAP-positive layer was measured by the average of three individual points in the cortex (Fig. 5A). When measuring the thickness of the GFAP-positive layer, the region of white matter was excluded from the measurement.

Neurological dysfunction was measured using three behavioral tests as follows: The von Frey test [11], the balance beam test [12], and the tail suspension test [13], with modifications. In the von Frey test, mice were placed in a wire mesh grid-based chamber (8 cm × 8 cm), and the contralateral hind paw was poked by a von Frey filament (0.008, 0.02, 0.04, or 0.07 g/cm^2) until the filament buckled. Poking was initiated with the thinnest filament (0.008 g/cm^2) before moving on to the next thinnest filament. The tension of the thinnest filament induced a positive response, which was considered the sensitivity threshold in the mouse. In the balance beam test, the number of stepping out of the forelimb and hindlimb on the contralateral side of the brain damage was counted as the mice crossed a 30 cm-long balance beam three times. In the tail suspension test, the mouse was lifted up by its tail by approximately 20 cm, and the number of times and the total length of time that it benched its body more than 10° off the vertical to the ipsilateral or contralateral side of the damaged hemisphere was measured over a period of 1 min. The percentage of the number of times (swing frequency) and the total length of time (swing time) to benching to the ipsilateral side against the total benching time were then calculated.

One-way analysis of variance (ANOVA) followed by Fisher's protected least significant difference test was used to examine the differences in the sequential change within the strain, and Student's unpaired *t*-test was used to examine for differences between strains. For correlations between the damage volume and area on the surface, the R^2 value was calculated by MS Excel (Microsoft, Washington, Redmond, WA, USA). A *P*-value <0.05 was considered significant.

Results

In the PIT-F model, damage was induced in the frontal lobe of the cortex, including a part of the motor area, the sensory area, and the association area, in both C57BL/6J (Fig. 1A) and BALB/c (Fig. 1B) mice [14]. The damage was induced not only in the cortex, but also in a small region of the striatum, which was comparable between C57BL/6J (Fig. 1C) and BALB/c mice (Figs. 1D, 3H, and 3I).

In this model, the damage size was also comparable between C57BL/6J and BALB/c mice on day 1 in terms of both the volume (Figs. 2B and C) and the area of the brain surface (Figs. 2D–F). Then, the damage decreased until day 21 in both strains (Figs. 2A–F). Meanwhile, the degree of decrease in the damage size was different between the two strains. The amount was larger on days 4, 14, and 21 in C57BL/6J mice compared to that in BALB/c mice, whereas it was comparable on day 7, as shown in the sections at the center of the damage (Fig.

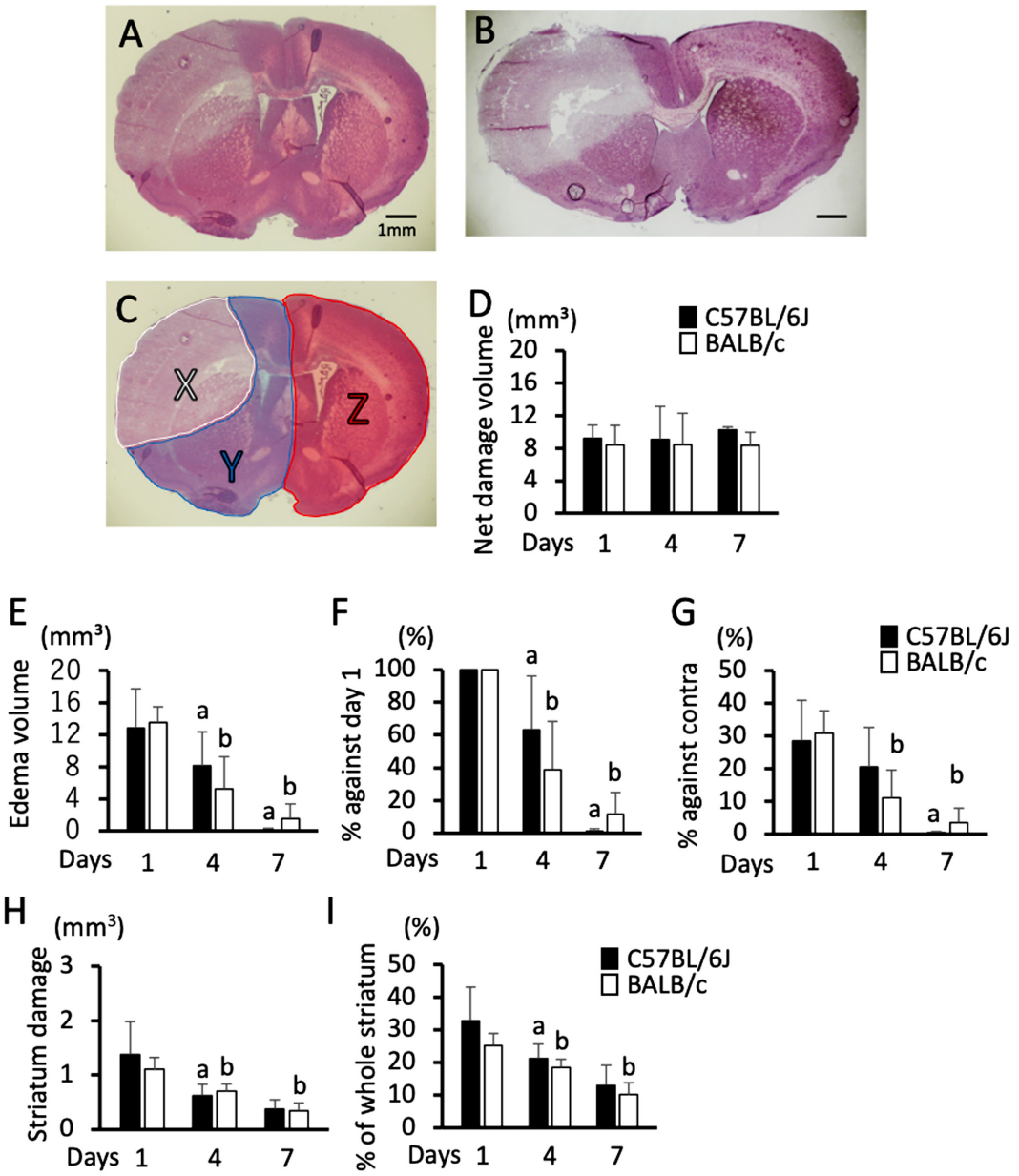

Fig. 3. Sequential change in net damage volume and edema volume from day 1 to day 7. A and B: Hematoxylin and eosin-stained brain section photomicrographs of C57BL/6J mice (A) and BALB/c mice (B) on day 1; bar indicates 1 mm. C: Partition of the brain section for the measurement of net damage and edema. Area-X, Y, and Z indicate the damaged area (X), ipsilateral alive area (Y), and contralateral area (Z) in the section shown in A. D: Sequential changes in net damage volume calculated by Z − Y. E–G: Sequential changes in edema volume calculated by X + Y − Z (E), percentage of edema volume against day 1 (F), and percentage of edema volume against contralateral hemisphere volume calculated by (X + Y − Z) / Z × 100 (G). H and I: Sequential changes in the size of striatum damage. Damage in terms of volume (H) and percentage of the whole striatum (I). Data represent the mean and SD. a: $P<0.05$ vs. day 1 in C57BL/6J mice, and b: $P<0.05$ vs. day 1 in BALB/c mice. n=6, 7, and 5 C57BL/6J mice, and n=6, 6, and 6 BALB/c mice were used on days 1, 4, and 7, respectively.

2A). Practically, the differences in the damage volume and percentage of volume against day 1 were significant on days 4, 14, and 21 (Figs. 2B and C). When the amount of damage was compared at the area on the surface, the size was also larger in C57BL/6J mice (Fig. 2D). This difference was significant on days 4, 14, and 21 (Fig. 2E). The difference in the area was significant on days 4, 14, and 21 (Fig. 2E), even though no significant difference was observed in the percentage of area against day 1 (Fig. 2F). Furthermore, the damage volume indicated remarkably high correlations with damage size on the brain surface in both C57BL/6J (Fig. 2G, R^2=0.916) and BALB/c mice (Fig. 2H, R^2=0.931).

Edema was prominent on day 1 in both C57BL/6J

 doi: 10.1538/expanim.20-0182

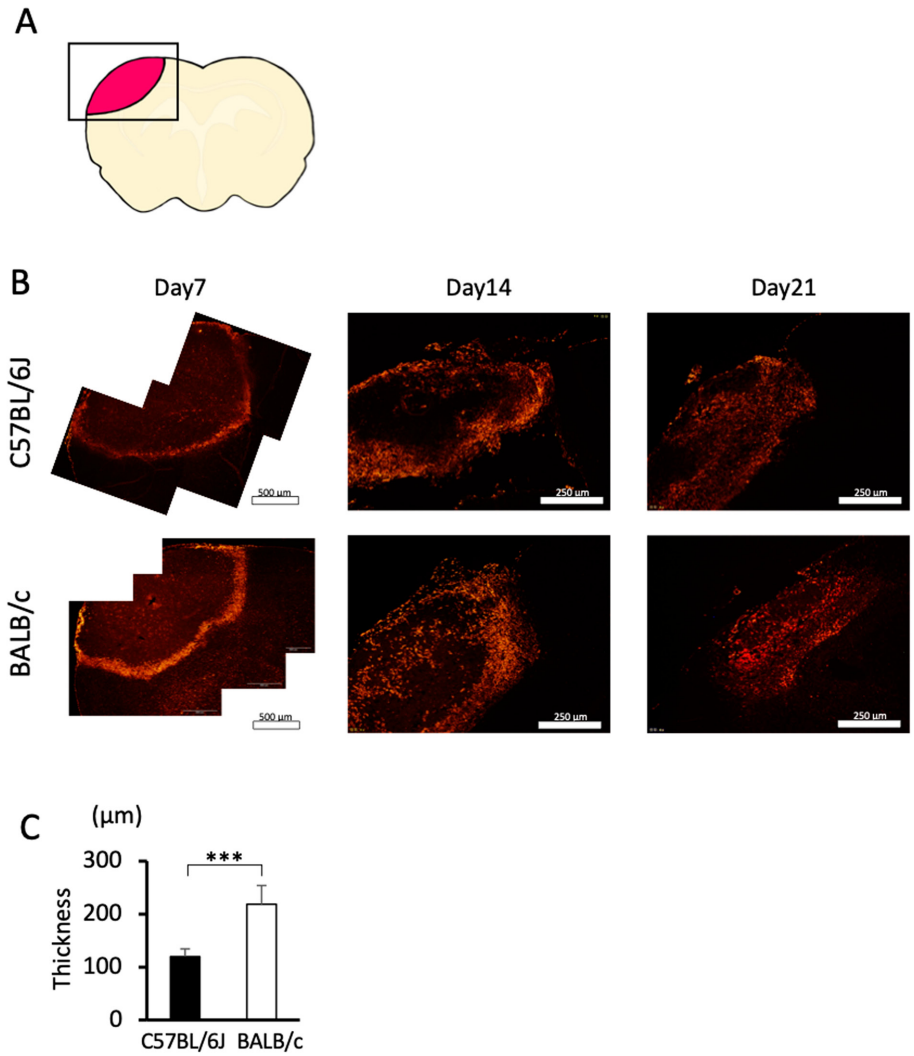

Fig. 4. Immunohistochemistry for F4/80. A: Picture of the brain section. A square indicates an analyzed area. B: Photomicrographs of F4/80-stained brain sections from C57BL/6J and BALB/c mice on days 7, 14, and 21. Bars indicate 500 μm on day 7, and 250 μm on days 14 and 21. C: Quantified thickness of the F4/80-positive layer surrounding the area of damage on day 7. Data represent the mean and SD. ***: P<0.001. Five C57BL/6J mice and six BALB/c mice were used on day 7. On days 14 and 21, 5 and 4 C57BL/6J mice and 6 and 4 BALB/c mice were analyzed, respectively. Comparable results were observed for each day and strain (data not shown).

(Fig. 3A) and BALB/c mice (Fig. 3B) in the PIT-F model. Therefore, we evaluated the sequential changes in the size of the net damage and edema. The net volume of damage did not change significantly until day 7 in either strain (Fig. 3D). Meanwhile, the edema was pronounced on day 1, decreased over time, and was almost abolished on day 7 after the induction of damage in both strains (Figs. 3E–G). This decrease was more remarkable in BALB/c mice than that in C57BL/6J mice from days 1 to 4, whereas it was comparable from days 4 to 7 (Figs. 3E–G). We also evaluated the area of damage in the stratum and found that it was comparable on day 1 and decreased similarly until day 7 in both strains (Figs. 3H and I).

To evaluate the accumulation of microglia after brain damage, we performed immunohistochemical analysis for F4/80, a marker of active microglia. The F4/80-positive microglia accumulated at the edge of the damaged region and formed a layer on day 7 (Fig. 4B), which was in line with previous observations [5]. We did not observe F4/80 immunoreactivity on days 1 or 4. Moreover, the thickness of the layer was significantly thinner in C57BL/6J mice than that in BALB/c mice (Fig. 4C). On days 14 and 21, F4/80 positive cells were distributed widely inside the damaged region in both strains (Fig. 4B). On day 14, these F4/80 positive cells were distributed relatively peripherally from the damaged region in C57BL/6J mice, whereas they were additionally distributed at the center of the damaged region in BALB/c mice. We observed comparable F4/80 immunoreactivity in both

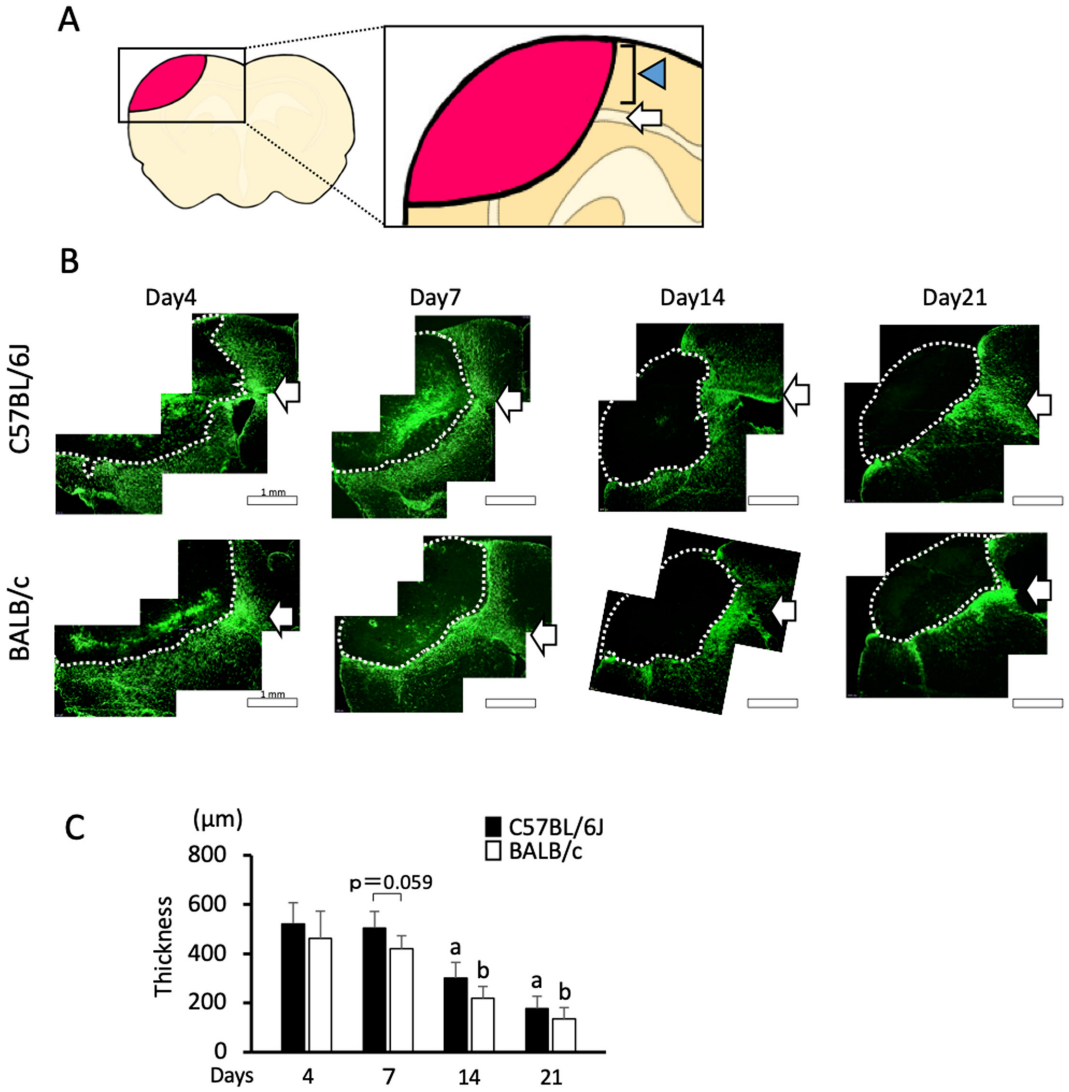

Fig. 5. Immunohistochemistry for GFAP. A: Picture of the brain section. A square indicates an analyzed area. The arrow indicates the white matter. Arrowhead indicates the cortex where the thickness is measured. B: Photomicrographs of GFAP-stained brain sections from C57BL/6J and BALB/c mice on days 7, 14, and 21. Dotted lines indicate the border of the damaged area. The arrows indicate white matter. Bars indicate 1 mm. C: Quantified thickness of the GFAP-positive layer surrounding the damaged area in the cortex on days 7, 14, and 21. Data represent the mean and SD. a: $P<0.05$ vs. day 1 in C57BL/6J mice b: $P<0.05$ vs. day 1 in BALB/c mice. n=5, 5, and 4 C57BL/6J mice were used on days 7, 14, and 21, respectively, and n=5, 5, and 5 BALB/c mice were used on days 7, 14, and 21, respectively.

strains of mice over the days examined (data not shown).

To evaluate the activation of astrocytes after brain damage, we performed immunohistochemical analysis for GFAP, a marker of reactive astrocytes. The GFAP-positive astrocytes formed a glial scar as a layer surrounding the damaged region on day 7 (Fig. 5B), which was also in line with previous observations [5]. A GFAP-positive signal in the white matter was continuously observed from day 4 until day 21 (Fig. 5B). Meanwhile, the thickness at the cortex was prominent on day 7 and decreased over time until day 21 (Figs. 5B and C). The thickness of the GFAP-positive layer in the cortex was comparable between the two strains on days 7, 14, and 21, even though there was a tendency for the layer to be thicker in C57BL/6J mice on day 7 (P=0.059).

We performed three different behavioral tests to evaluate neurological dysfunction. In the von Frey test, which evaluates sensory function [11], both strains showed a significant increase in the sensory threshold on day 1, which was more remarkable in C57BL/6J mice than that in BALB/c mice, and had recovered to a normal level by day 7 (Fig. 6A). In the balance beam test, which evaluates the motor function of contralateral limbs [12], the number of stepping-off was significantly increased on days 2 and 5 in the forelimb and on days 2, 7, 14, and 21 in the hind limb in C57BL/6J mice, whereas on day

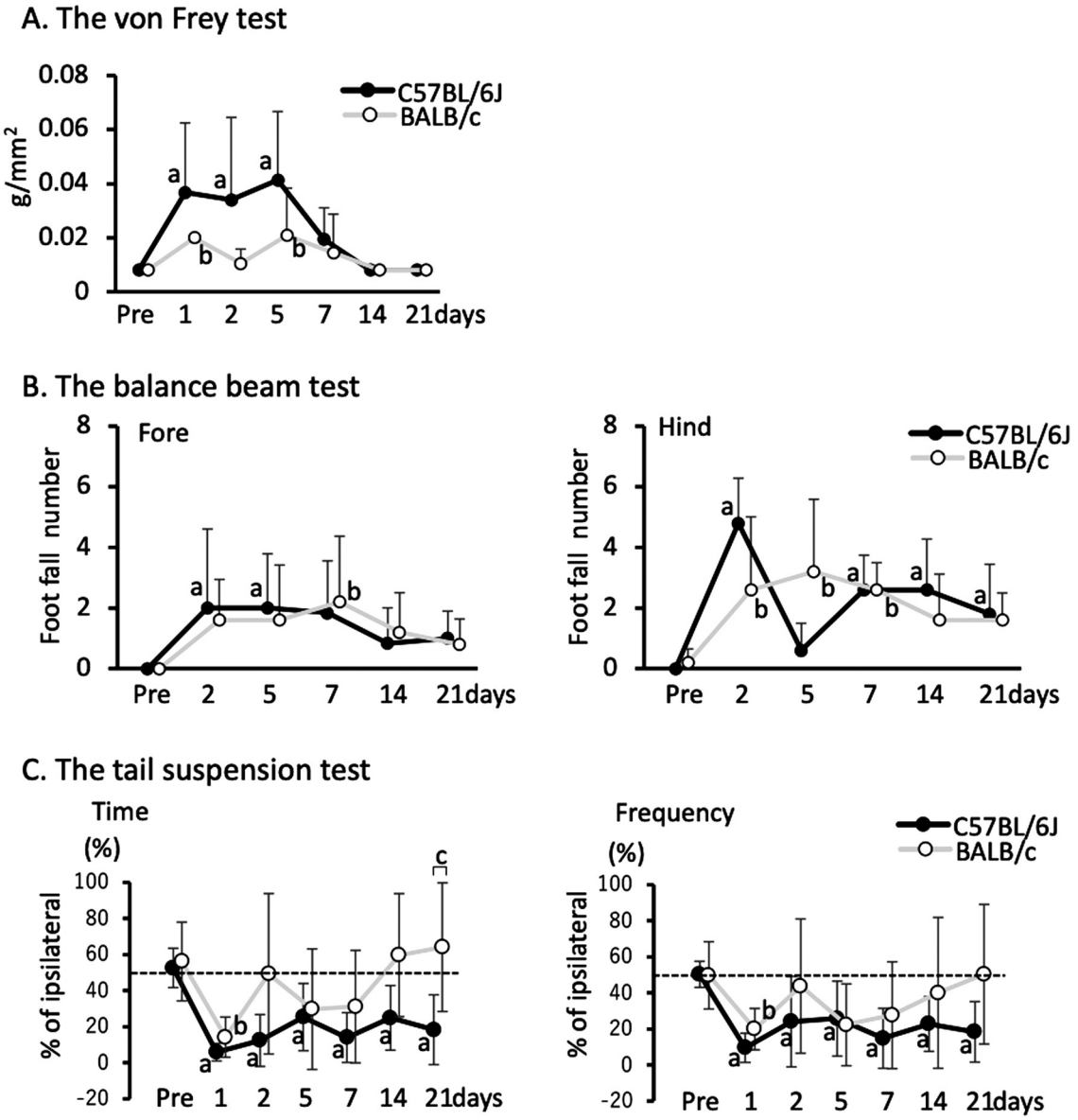

Fig. 6. Sequential changes in neurological dysfunction after brain damage in C57BL/6J and BALB/c mice. A: Sensitivity threshold of the contralateral hind paw in the von Frey test. B: The numbers of foot-falling in the contralateral forelimb and hindlimb in the balance beam test. C: Percentage of body swing time and frequency in the tail suspension test. Data represent mean and SD. a: $P<0.05$ vs. Pre in C57BL/6J mice, b: $P<0.05$ vs. Pre in BALB/c mice, c: $P<0.05$ comparison between C57BL/6J and BALB/c mice. Six C57BL/6J mice and five BALB/c mice were used.

7 in the forelimb and on days 2, 5, and 7 in the hind limb in BALB/c mice compared with the level before damage (Fig. 6B). This test was not performed on day 1 because of the remarkable reduction in spontaneous locomotion activity in mice, which likely a resulted of surgery. In the tail suspension test, which evaluates the deviation of motor function in each hemibody [13], both the time and frequency of body suspension significantly deviated to the contralateral side on day 1. Deviations were continuously observed until day 21 in C57BL/6J mice, but disappeared on day 2 in BALB/c mice. In particular, the difference in body suspension time was significant between strains on day 21 (Fig. 6C).

Discussion

In this study, we demonstrate that the PIT-F model is capable of inducing brain damage with small variation between individual animals and different strains, similar to the PIT-P model. This damage was associated with neurological dysfunction, as determined by three behavioral tests. Furthermore, pathophysiological responses after stroke, including edema, microglial accumulation, and astrocyte activation, were also observed in this model, indicating that the model induced pathophysiological responses comparable to those in existing models. Although many animal stroke models associated with

neurological dysfunction have been established, most of them have relatively large variations in stroke outcome [1–3]. Our previous finding showed that the initial amount of damage influences the induction of subsequent repair responses [5]. Unlike other animal stroke models with large variations that are unsuitable for studying pathological processes after damage, the current model is suitable for studying pathophysiological responses, the recovery of neurological dysfunction, and their relationship after stroke.

In the PIT-F model, the surface area of the damage was highly correlated with the volume of the damage. This high correlation may be due to the fact that the damage in the PIT-F and PIT-P models is induced in the light-reachable area by photochemical reaction. Therefore, the amount of damage can be evaluated from the damaged area on the surface of the brain in these models.

We also found that the reduction in damage after stroke induction was different between C57BL/6J and BALB/c mice, even though the initial amounts of damage were comparable. The reduction in edema was more prominent in BALB/c mice than that in C57BL/6J mice from day 1 to day 4, whereas it was comparable from day 4 to day 7. Given that it has been reported that the amount of cerebral blood flow is lower in C57BL/6J mice than that in BALB/c mice [15], the reduction in edema by the clearance of intra/intercellular fluid in the edema region with blood flow may occur slower in C57BL/6J mice than that in BALB/c mice.

The granular layer, composed of F4/80-positive reactive microglia, was thinner in C57BL/6J mice than that in BALB/c mice on day 7. Since phagocytosis by microglia is involved in the reduction of brain infarction in ischemic stroke [16], the reduced accumulation of microglia in C57BL/6J mice likely resulted in a later reduction in damage compared to that in BALB/c mice after day 7. In addition, reactive microglia were more remarkable in the center of the damaged region on day 14, suggesting that they are activated to a greater extent in BALB/c mice than that in C57BL/6J mice. As it is known that microglial accumulation after ischemic stroke is regulated by macrophage chemoattractant protein 1 [17], its induction might be lower in C57BL/6J mice than that in BALB/c mice. Since the F4/80-positive microglia were widely distributed inside the damaged region on days 14 and 21 in both strains, the difference in the amount of damage on days 14 and 21 might have resulted from the difference in the activation of microglia on day 7.

The layer of glial scar composed of GFAP-positive activated astrocytes tended to be thicker in C57BL/6J mice than that in BALB/c mice on day 7 (P=0.059). The glial scar functions as a “wall” to protect intact brain tissue from harmful factors as a result of tissue damage [18]. It is known that several signaling molecules, including transforming growth factor, ciliary neurotrophic factor, interleukin-6, leukemia inhibitory factor, and oncostatin M, trigger astrocyte activation [19]. Therefore, the difference in astrocyte activation between the strains may have resulted from the difference in one or more of these molecules.

In the PIT-F model, brain damage was associated with neurological dysfunctions, which likely resulted in damage to the sensory, motor, and association regions in the cortex. Therefore, this model is also useful for assessing the recovery of neurological dysfunction after ischemic stroke. In the current study, the neurological dysfunction recovered, at least partially, over time. Both neuronal loss and functional impairment of neurons are considered to cause neurological dysfunction. We also found that the net amount of damage was comparable from day 1 to day 7 in both strains, and neuronal loss reached the maximum level on day 1 in this model. Therefore, the recovery from day 1 to day 21 was not associated with the ratio of neuronal loss. The neurological dysfunction caused by functional impairment of neurons can be recovered by the improvement of these neurons. Since edema of the damaged region compresses the surrounding tissue and leads to neuronal impairment [20], its improvement is likely to assist with the recovery of neurological dysfunction. In this model, edema was reduced until day 7; therefore, the recovery of neurological dysfunction at day 7 may be associated with the improvement of edema. The neurological dysfunction can be recovered by neural network reconstruction with neurogenesis or network remodeling. Neurogenesis is noticeable 3 weeks after the induction of damage [21], and neural network reconstruction is thought to be mainly attributed to network remodeling until day 21. Reconstruction for functional improvement can occur near the damaged region but also in the region further away, including the spinal cord [22]. The involvement of edema reduction and neural network reconstruction in the recovery of neurological dysfunction is poorly understood. The relatively large variation in both the amount of damage and the subsequent pathophysiological responses in the existing stroke models makes analysis difficult. Therefore, their involvement should be clarified with this model.

We also found that the recovery of both neurological dysfunctions and repair reactions was different between the two strains, in that dysfunction was relatively more severe, and the repair reactions recovered later in C57BL/6J mice than that in BALB/c mice. These differ-

ences between strains should be taken into account when the recovery of neurological dysfunction is assessed in transgenic/knockout mice with different genetic backgrounds. One potential explanation for these differences is that the distribution of the motor, sensory, and association areas in the cortex varies between strains, and comparable damage induction might cause different degrees of damage in each area. Another possibility is that the recovery responses to neurological dysfunction are different between stains. Indeed, the improvement in edema, which impairs neurological dysfunction, was more prominent in BALB/c mice than that in C57BL/6J mice from days 1 to 4, whereas it was comparable on days 4 to 7, which may have resulted in the later recovery of neurological dysfunction in C57BL/6J mice than that in BALB/c mice. In addition, F4/80-positive microglial accumulation was more prominent in BALB/c mice than that in C57BL/6J mice on day 7. Considering that microglia accelerate neuronal plasticity [23], the more prominent accumulation of microglia in BALB/c mice may be involved in the recovery of neurological dysfunction. Furthermore, the layer of GFAP-positive reactive astrocytes in the cortex tended to be thinner in BALB/c mice than in C57BL/6J mice. Given that reactive astrocytes secrete chondroitin sulfate proteoglycans, which inhibit axonal outgrowth [24], more astrocyte activation in the cortex in C57BL/6J mice than that in BALB/c mice might result in less reconstruction of the neural network in the surrounding region to facilitate improvements in neurological dysfunction. These possibilities should be clarified by further studies.

Acknowledgments

This study was supported by a Grant-in-Aid for Scientific Research (C) (grant 15K08194) and MEXT-Supported Program for the Strategic Research Foundation at Private Universities (grant 1201037) by the Ministry of Education, Culture, Sports, Science, and Technology.

We would like to thank Editage (www.editage.com) and Dr. Kiyo Sakagami for English language editing.

References

1. Fujie W, Kirino T, Tomukai N, Iwasawa T, Tamura A. Progressive shrinkage of the thalamus following middle cerebral artery occlusion in rats. Stroke. 1990; 21: 1485–1488. [Medline] [CrossRef]
2. Koizumi J, Nakazawa T, Ooneda G. Experimental studies of ischemic brain edema. I. A new experimental model of cerebral embolism in rats in which recirculation can be introduced in the ischemic area. Jpn J Stroke. 1986; 8: 1–8. [CrossRef]
3. Umemura K, Wada K, Uematsu T, Nakashima M. Evaluation of the combination of a tissue-type plasminogen activator, SUN9216, and a thromboxane A2 receptor antagonist, vapiprost, in a rat middle cerebral artery thrombosis model. Stroke. 1993; 24: 1077–1081, discussion 1081–1082. [Medline] [CrossRef]
4. Majid A, He YY, Gidday JM, Kaplan SS, Gonzales ER, Park TS, et al. Differences in vulnerability to permanent focal cerebral ischemia among 3 common mouse strains. Stroke. 2000; 31: 2707–2714. [Medline] [CrossRef]
5. Nagai N, Kawao N, Okada K, Ishida C, Okumoto K, Ueshima S, et al. Initial brain lesion size affects the extent of subsequent pathophysiological responses. Brain Res. 2010; 1322: 109–117. [Medline] [CrossRef]
6. Zhang H, Prabhakar P, Sealock R, Faber JE. Wide genetic variation in the native pial collateral circulation is a major determinant of variation in severity of stroke. J Cereb Blood Flow Metab. 2010; 30: 923–934. [Medline] [CrossRef]
7. Chan PH, Epstein CJ, Li Y, Huang TT, Carlson E, Kinouchi H, et al. Transgenic mice and knockout mutants in the study of oxidative stress in brain injury. J Neurotrauma. 1995; 12: 815–824. [Medline] [CrossRef]
8. Nagai N, De Mol M, Lijnen HR, Carmeliet P, Collen D. Role of plasminogen system components in focal cerebral ischemic infarction: a gene targeting and gene transfer study in mice. Circulation. 1999; 99: 2440–2444. [Medline] [CrossRef]
9. Yano M, Kawao N, Tamura Y, Okada K, Ueshima S, Nagai N, et al. Spatiotemporal differences in vascular permeability after ischaemic brain damage. Neuroreport. 2011; 22: 424–427. [Medline] [CrossRef]
10. Yao X, Derugin N, Manley GT, Verkman AS. Reduced brain edema and infarct volume in aquaporin-4 deficient mice after transient focal cerebral ischemia. Neurosci Lett. 2015; 584: 368–372. [Medline] [CrossRef]
11. Wu J, Su G, Ma L, Zhang X, Lei Y, Li J, et al. Protein kinases mediate increment of the phosphorylation of cyclic AMP-responsive element binding protein in spinal cord of rats following capsaicin injection. Mol Pain. 2005; 1: 26. [Medline] [CrossRef]
12. Luong TN, Carlisle HJ, Southwell A, Patterson PH. Assessment of motor balance and coordination in mice using the balance beam. J Vis Exp. 2011; 10: 2376. [Medline]
13. Ritzel RM, Patel AR, Spychala M, Verma R, Crapser J, Koellhoffer EC, et al. Multiparity improves outcomes after cerebral ischemia in female mice despite features of increased metabovascular risk. Proc Natl Acad Sci USA. 2017; 114: E5673–E5682. [Medline] [CrossRef]
14. Franklin BJK, Paxinos G. The mouse brain in the stereotaxic coordinate. 3rd ed. ed. London: Elsevier; 2008.
15. Kang HM, Sohn I, Kim S, Kim D, Jung J, Jeong JW, et al. Optical measurement of mouse strain differences in cerebral blood flow using indocyanine green. J Cereb Blood Flow Metab. 2015; 35: 912–916. [Medline] [CrossRef]
16. Schroeter M, Jander S, Huitinga I, Witte OW, Stoll G. Phagocytic response in photochemically induced infarction of rat cerebral cortex. The role of resident microglia. Stroke. 1997; 28: 382–386. [Medline] [CrossRef]
17. Hughes PM, Allegrini PR, Rudin M, Perry VH, Mir AK, Wiessner C. Monocyte chemoattractant protein-1 deficiency is protective in a murine stroke model. J Cereb Blood Flow Metab. 2002; 22: 308–317. [Medline] [CrossRef]
18. Silver J, Miller JH. Regeneration beyond the glial scar. Nat Rev Neurosci. 2004; 5: 146–156. [Medline] [CrossRef]
19. Pekny M, Wilhelmsson U, Tatlisumak T, Pekna M. Astrocyte activation and reactive gliosis-A new target in stroke? Neurosci Lett. 2019; 689: 45–55. [Medline] [CrossRef]
20. Kubis N. Non-invasive brain stimulation to enhance post-stroke recovery. Front Neural Circuits. 2016; 10: 56. [Medline] [CrossRef]
21. Yamashita T, Ninomiya M, Hernández Acosta P, García-Verdugo JM, Sunabori T, Sakaguchi M, et al. Subventricular

zone-derived neuroblasts migrate and differentiate into mature neurons in the post-stroke adult striatum. J Neurosci. 2006; 26: 6627–6636. [Medline] [CrossRef]
22. Ueno M, Hayano Y, Nakagawa H, Yamashita T. Intraspinal rewiring of the corticospinal tract requires target-derived brain-derived neurotrophic factor and compensates lost function after brain injury. Brain. 2012; 135: 1253–1267. [Medline] [CrossRef]
23. Lartey FM, Ahn GO, Ali R, Rosenblum S, Miao Z, Arksey N, et al. The relationship between serial [(18)F]PBR06 PET imaging of microglial activation and motor function following stroke in mice. Mol Imaging Biol. 2014; 16: 821–829. [Medline] [CrossRef]
24. Smith GM, Strunz C. Growth factor and cytokine regulation of chondroitin sulfate proteoglycans by astrocytes. Glia. 2005; 52: 209–218. [Medline] [CrossRef]